JACS
JOURNAL OF THE AMERICAN CHEMICAL SOCIETY
Article
pubs.acs.org/JACS

Ion Pair Dynamics: Solvolyses of Chiral 1,3-Diarylallyl Carboxylates as a Case Study

Konstantin Troshin and Herbert Mayr*

Department Chemie, Ludwig-Maximilians-Universität München, Butenandtstrasse 5-13 (Haus F), 81377 München, Germany

Supporting Information

ABSTRACT: Chiral ion pairs play a key role in modern enantioselective synthesis, though little is known about their properties. We have now used the special features of unsymmetrically substituted allyl derivatives to obtain unprecedented insight into ion pair dynamics. By employing chiral high-performance liquid chromatography, it was possible to follow the time-dependent concentrations of all four isomeric esters (two regioisomeric pairs of enantiomers) and all four isomeric alcohols generated during the hydrolysis of enantiopure 1-(4-chlorophenyl)-3-phenylallyl and 3-(4-chlorophenyl)-1-phenylallyl 4-nitrobenzoates. Combination of these results with the directly measured rate constant for the reaction of the laser-flash photolytically generated 1-(4-chlorophenyl)-3-phenylallyl cation with water provided a complete mechanistic scheme for allyl carboxylate solvolysis. It is demonstrated that solvolysis and internal return can be explained by the same intermediates. The correlation equation $\log k = s_N(N + E)$ was used to elucidate the variable importance of external and internal return in the solvolysis reactions. This information will be crucial for the interpretation of the ultrafast dynamics of ion pairs generated by femtosecond laser pulses.

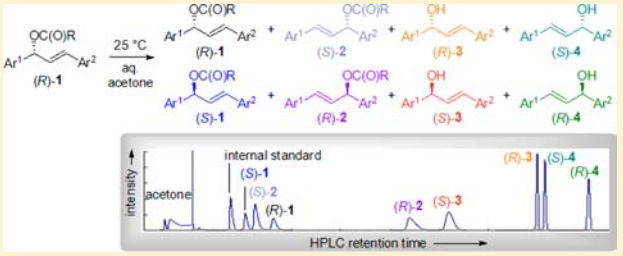

INTRODUCTION

Control of enantioselectivity by noncovalent interactions has become a major tool in organic synthesis. In particular hydrogen-bonding, as in thiourea-catalyzed reactions,[1] and ion-pairing[2] have extensively been used for stereoselective transformations. An early example for the use of ion-pairing in asymmetric synthesis was reported by Dolling et al.,[3] who found that a cinchona-derived quaternary ammonium ion salt can be employed as catalyst for the asymmetric methylation of a substituted indanone under phase-transfer conditions. That pioneering work opened the field of asymmetric phase-transfer catalysis, the scope of which has widely been elaborated by Maruoka and associates.[4] Protonation of organic substrates by strong chiral Brønsted acids, in particular BINOL-derived phosphoric acid diesters and their derivatives, gives rise to chiral ion pairs or similar structures, which serve as chiral electrophiles in a manifold of reactions,[5] including enantioselective cycloadditions,[6] electrocyclic reactions,[7] 1,4-additions,[8] Friedel−Crafts allylations,[9] reductions,[10] and ene reactions.[11] Hydrogen-bonding between the resulting cation and the chiral counteranion often provides additional stabilization of the positively charged electrophilic intermediate and accounts for the augmented enantioselectivity. In some cases it is difficult to differentiate whether chirality is induced by ion-pairing of an achiral cationic electrophile with a chiral counteranion or by activation of neutral electrophiles (e.g., imines or carbonyl compounds) through hydrogen-bonding with a chiral Brønsted acid.[12]

However, treatment of prochiral substrates with strong chiral Brønsted acids is not the only method to generate chiral ion pairs for asymmetric counterion-directed synthesis.[2,13] Ion-pairing was also employed in enantioselective iminium-activated reactions by using achiral ammonium ions with chiral counterions[14] as well as in various asymmetric transition-metal-catalyzed reactions, which utilized the directing effect of chiral counteranions.[15] Ooi demonstrated that transition metal complexes with achiral ligands carrying a quaternary onium moiety can be electrostatically bound to chiral anions to induce asymmetrical palladium catalysis.[16] The general importance of ion-pairing in transition metal-catalyzed reactions has been reviewed by Macchioni, who suggested that ion-pairing should be considered as one of the instruments for tuning catalytic processes.[17]

Enantioselective catalysis was furthermore achieved by combining ion-pairing with hydrogen-bonding. Examples are reactions catalyzed by chiral ureas which are coordinated to achiral counterions[18] as well as cooperative catalysis, where hydrogen-bonding was used to link the complex counterion to the active intermediate, thus providing additional attractive forces within the ion pair.[19] Extensive studies on the role of ion-pairing in carbocationic polymerizations have recently been reviewed by Bochmann.[20]

While the targeted use of ion-pairing in enantioselective synthesis and polymerization reactions thus reflects recent

Received: August 31, 2012
Published: November 28, 2012

dx.doi.org/10.1021/ja308670g | J. Am. Chem. Soc. 2013, 135, 252−265

developments, the importance of ion-pairing for organic reactivity had already been recognized in the 1950s by Winstein and co-workers. Their studies of S_N1 solvolyses[21] provided the basis of our current understanding of ion pairs and their reactivities.[22] Because of their ability to undergo allylic rearrangements, allyl derivatives turned out to be particularly valuable systems for gaining insight into the nature and reactivity of ion pairs.[21a,22,23] Goering's pioneering investigations of the transformations of optically active allyl derivatives by titrimetric and polarimetric methods as well as product analyses including isotope exchange experiments have become textbook examples[24] to demonstrate the role of ion-pairing in S_N1 reactions.

Since the *cis*/*trans* isomerization of optically active *cis*- and *trans*-5-methylcyclohex-2-enyl 2-carboxybenzoates (**A**⇌**B**, LG = OPht, Scheme 1) in acetonitrile was found to proceed significantly more slowly than the racemization ((*S*)-**A**⇌(*R*)-**A**; (*S*)-**B**⇌(*R*)-**B**),[25] Goering proposed the formation of ion pair intermediates (**C**, **D**), in which the anion remains on the same face of the allyl cation as in the substrate. The collapse of these ion pairs (internal return) either regenerates the starting materials or leads to their enantiomers by attack of the anion at the other allylic terminus. The *cis*/*trans* isomerization, which requires the migration of the leaving group (LG) to the other face of the allyl cation, was proposed to proceed via dissociation of the initial ion pairs to an achiral carbocationic intermediate (**E**) that can be attacked by the LG from both faces (Scheme 1).[25]

Scheme 1. Ion Pair Mechanism Proposed by Goering for Solvolyses and Rearrangements of *cis*- and *trans*-5-Methylcyclohex-2-enyl Derivatives[a]

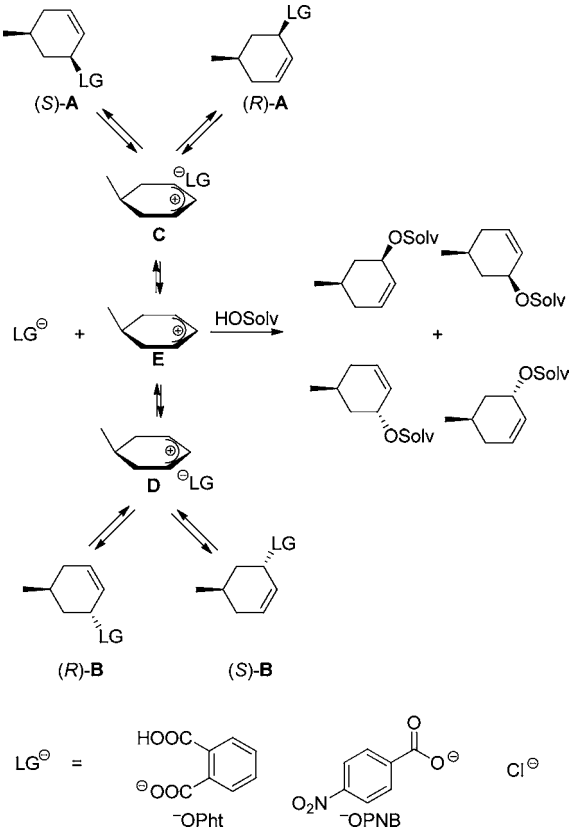

[a]The descriptors (*R*) and (*S*) for the configuration of C-5 (connected to the methyl group) are omitted.

The hydrolyses of *cis*- and *trans*-5-methylcyclohex-2-enyl 2-carboxybenzoates (**A**, **B**, LG = OPht)[26] and 4-nitrobenzoates (**A**, **B**, LG = OPNB)[27] in aqueous acetone as well as the ethanolyses and acetolyses of *cis*- and *trans*-5-methylcyclohex-2-enyl chlorides (**A**, **B**, LG = Cl)[28] were rationalized on the basis of this mechanism. In none of these cases was *cis*/*trans* isomerization of the non-reacted substrates detected, and the polarimetric rate constant (racemization plus solvolysis) was always larger (factor of 1.1−5.07) than the titrimetric rate constant (solvolysis only).

In contrast to the situation described for symmetrical allyl systems in Scheme 1, racemization of unsymmetrical allyl derivatives implies migration of the LG to the other face of the allyl cation. As solvolyses of *trans*-3-methyl-1-phenylallyl and *trans*-1-methyl-3-phenylallyl 4-nitrobenzoates in aqueous acetone were later observed to be accompanied by approximately 70% racemization of the unsolvolyzed esters, Goering concluded that the previously investigated stereochemical behavior of cyclohexenyl derivatives (Scheme 1) was largely dominated by conformational phenomena, which are absent in acyclic derivatives.[29] Therefore, the stereochemistry of S_N1 reactions of acyclic allyl derivatives, which is crucial for understanding ion-pairing in general, has not been clarified conclusively up to the present time.

Winstein's ion pair mechanism (Scheme 2),[30] which has commonly been used to rationalize the course of solvolysis reactions through the intermediacy of contact ion pairs (CIPs), solvent-separated ion pairs (SSIPs), and free ions, has recently been employed to interpret the picosecond dynamics of laser-flash-generated CIPs.[31]

Scheme 2. Classical Winstein Scheme for Solvolysis Reactions[30]

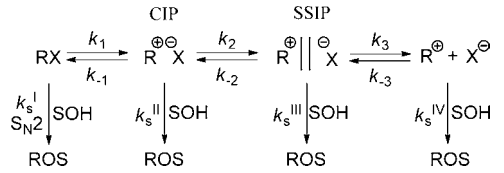

It is commonly assumed that such photolytically generated CIPs, which may be formed either directly as the initial cleavage products or through electron transfer in the initially generated geminate radical pairs, are similar to the intermediates in solvolysis reactions.[31] Vice versa, the rates measured for geminate recombinations of laser-flash photolytically generated ion pairs were used to discuss structural effects on the rates of internal return during the solvolytic reactions.[32]

However, Winstein's solvolysis scheme includes many parameters which could not be unambiguously differentiated with the analytical methods available at that time, so many questions remained open. It is still unclear, for example, whether solvolysis and internal return proceed through the same intermediates or are two independent processes involving different types of ion pairs.[33]

A crucial step toward a quantitative description of solvolysis reactions, and of nucleophilic aliphatic substitutions in general, was taken in the investigations by Jencks, Richard, and Tsuji,[34−36] who used clock methods to determine rate constants for the attack of solvents on the intermediate

dx.doi.org/10.1021/ja308670g | J. Am. Chem. Soc. 2013, 135, 252−265

carbocations. They were able to not only identify the change from S_N1 to S_N2 mechanisms[34] but also clarify the dynamics of ion pair dissociation[35] and recombination.[36]

By introducing stopped-flow techniques for determining rates of solvolysis reactions, which occur in the millisecond to second time domain,[37] and systematic extension of the data set for the rates of the reactions of carbocations with solvents[38] and other nucleophiles,[39] we arrived at linear free energy relationships,[39,40] which allow one to predict changes in solvolysis mechanisms as the substrates and solvents are altered.[41] Under the same conditions, increasing stabilization of the carbocations led to the change from S_N2 reactions, over S_N1 reactions without and with common ion return, to S_N2C^+ processes (formation of carbocation occurs faster than its reaction with the solvent) and heterolytic cleavages of esters, which proceed with formation of persistent carbocations.[41] Furthermore, we recently employed femtosecond spectroscopy to investigate the dynamics of free and paired carbocations on the picosecond time scale in collaboration with the Riedle group.[42]

Combination of all these techniques has provided detailed information about the whole range of carbocation reactivities[37,43]—from very slow reactions to those occurring within ion pairs which proceed at rates approaching vibrational frequencies. On the other hand, our knowledge about structures and dynamics of intramolecular interconversions of ion pairs has remained crude.

We therefore approached the dynamics of ion pair transformations by taking advantage of the special properties of allylic derivatives described above. While titrimetry and polarimetry were the most important analytical tools available to Goering for studying the course of the solvolysis reactions, we could now employ chiral high-performance liquid chromatography (HPLC) techniques to obtain unprecedented insight into the course of S_N1 reactions and ion-pairing.

When the enantiopure esters (*R*)-**1** and (*S*)-**2** were dissolved in aqueous acetone (for structures, see Scheme 3), mixtures of four isomeric allyl alcohols (hydrolysis products) and four isomeric allyl 4-nitrobenzoates (starting material and products of ion recombination) were obtained. As we succeeded in separating these eight compounds by HPLC, it was possible to follow the changes in concentration of each of these individual compounds as a function of time and to develop a kinetic model that quantitatively describes the whole mechanistic scheme. As we report individual rate constants for interconversions between covalent substrates, ion pairs, and free ions, this work can be considered a bridge between the classical solvolysis studies from the 1950s to 1970s and modern applications of ion-pairing in stereoselective organic synthesis and their role in photosolvolytic processes. We can thus not only answer questions that remained open when our knowledge of ion-pairing effects in solvolysis reactions was mostly derived from the difference between polarimetric and titrimetric rate constants, but also provide the basis for the interpretation of ultrafast dynamics of ion pairs generated by femtosecond laser pulses.

RESULTS

Synthesis and Chromatographic Separation of the Model Compounds. The regioisomeric alcohols *rac*-**3** and *rac*-**4** were obtained by $NaBH_4$ reduction of the corresponding chalcones according to ref 44. Sharpless kinetic resolution[45] of *rac*-**3** and *rac*-**4** using D- or L-diisopropyl tartrate (D-/L-DIPT), respectively, followed by treatment with 4-nitrobenzoyl chloride in the presence of triethylamine and recrystallization, gave the enantiopure (ee >99%, HPLC) allylic esters (*R*)-**1** and (*S*)-**2** (Scheme 3).

Scheme 3. Synthesis of the Enantiopure Allylic Esters (*R*)-1 and (*S*)-2[a]

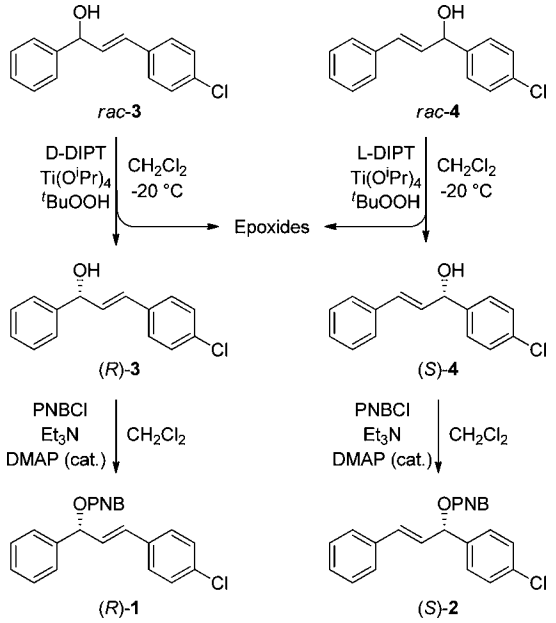

[a]PNB = 4-nitrobenzoyl, DIPT = diisopropyl tartrate, DMAP = 4-(dimethylamino)pyridine.

As treatment of either (*R*)-**1** or (*S*)-**2** with aqueous acetone may give a mixture of four esters [(*R*)-**1**, (*S*)-**1**, (*R*)-**2**, and (*S*)-**2**] and four alcohols [(*R*)-**3**, (*S*)-**3**, (*R*)-**4**, and (*S*)-**4**], a complete analysis of the solvolysis mechanism requires monitoring the concentrations of eight compounds.

Figure 1 shows that mixtures of the racemic compounds **1**–**4** can be resolved using chiral HPLC (eight peaks in total), which gives the unique possibility of following the time-dependent changes in concentration of the individual enantiomers.

Kinetic Experiments. *General.* The 4-nitrobenzoates **1** and **2** were solvolyzed in aqueous acetone at 25 °C with and

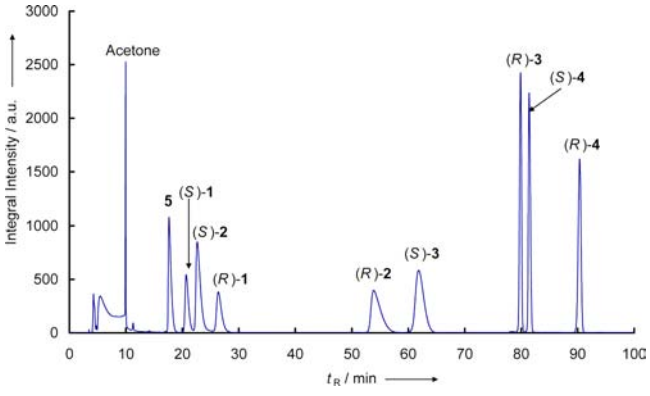

Figure 1. Chromatogram of an artificial mixture of racemic **1**–**4** and (*E*)-1-(4-methylphenyl)-3-phenylprop-2-en-1-one (**5**) (internal standard). Details of the HPLC method are described in the Supporting Information.

dx.doi.org/10.1021/ja308670g | J. Am. Chem. Soc. 2013, 135, 252–265

Table 1. Summary of the HPLC Kinetic Experiments

entry	solvent	substrate	$[substrate]_0$/M	additive	$[additive]_0$/M
1	60% aq acetone	(*R*)-**1**	1.53×10^{-3}		
2	60% aq acetone	(*R*)-**1**	8.04×10^{-4}	Bu_4NOPNB^a	4.82×10^{-3}
3	60% aq acetone	(*R*)-**1**	7.82×10^{-4}	Bu_4NOPNB^a	5.25×10^{-2}
4	60% aq acetone	(*R*)-**1**	8.04×10^{-4}	NaN_3	7.08×10^{-2}
5	60% aq acetone	(*R*)-**1**	1.02×10^{-3}	Bu_4NCl	1.87×10^{-2}
6	60% aq acetone	(*R*)-**1**	8.51×10^{-4}	Bu_4NCl	1.01×10^{-1}
7	60% aq acetone	(*R*)-**1**	8.70×10^{-4}	piperidine	5.42×10^{-2}
8	60% aq acetone	(*R*)-**1**	8.61×10^{-4}	$LiClO_4$	9.46×10^{-3}
9	60% aq acetone	(*S*)-**2**	7.85×10^{-4}		
10	60% aq acetone	(*S*)-**2**	7.90×10^{-4}	NaN_3	7.66×10^{-2}
11	80% aq acetone	(*R*)-**1**	7.72×10^{-4}		
12	90% aq acetone	(*R*)-**1**	6.82×10^{-4}		

[a]Tetrabutylammonium 4-nitrobenzoate.

without addition of various nucleophiles. The experiments are summarized in Table 1.

Aliquots of the reaction mixtures were extracted with dichloromethane or diethyl ether after certain time intervals, followed by HPLC analysis. A typical chromatogram obtained during such an experiment is shown in Figure S1 in the Supporting Information. By using (*E*)-1-(4-methylphenyl)-3-phenylprop-2-en-1-one (**5**) as internal standard, we determined the time-dependent yields for all compounds present in the mixture.

Solvolyses of (R)-1 and (S)-2 in 60% Aqueous Acetone. Figure 2 shows that both regioisomeric alcohols **3** and **4** are formed as racemates during the solvolysis of (*R*)-**1** in 60% aqueous acetone. The marginal separation of the graphs for (*R*)-**3** and (*S*)-**3** can be explained by the different shapes of their HPLC signals and the drift of the baseline caused by the gradient used to shorten the overall elution time. As no isomerization was detectable within 2.75 h when (*S*)-**4** was dissolved in 60% aqueous acetone containing 2 mM 4-nitrobenzoic acid (the highest concentration of the acid which can be present at the end of the solvolyses under the experimental conditions used), one can exclude enantioselective formation of **3** and **4** and subsequent isomerization. In line with this observation, the ratio [**3**]/[**4**] = 1.5 remained constant throughout the reaction. Therefore, an S_N2 mechanism as well as nucleophilic trapping of the chiral CIPs by water prior to racemization (steps with k_s^I and k_s^{II} in the classical Winstein scheme[30]) can be excluded for this system: both pathways would result in the formation of enantioenriched products (complete or partial inversion of configuration).

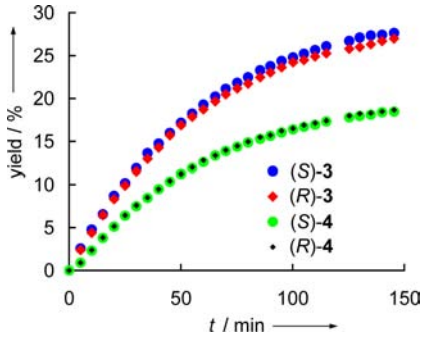

Figure 2. Time-dependent yields of **3** and **4** during the solvolysis of (*R*)-**1** (1.5 mM) in 60% aqueous acetone at 25 °C.

Figure 3 shows that the consumption of (*R*)-**1** leads not only to the formation of the hydrolysis products **3** and **4** discussed above but also to the intermediate appearance of the isomeric 4-nitrobenzoates (*S*)-**2**, (*S*)-**1**, and (*R*)-**2**.

The prevailing formation of (*S*)-**2** indicates that the LG stays preferentially at the same face of the plane of the allyl cation, which implies that allylic rearrangement occurs predominantly at the CIP stage.

Solvolysis of (*S*)-**2** in 60% aqueous acetone followed exactly the same pattern as solvolysis of (*R*)-**1** in the same solvent. Both alcohols **3** and **4** were formed as racemates, and the ratio [**3**]/[**4**] = 1.5 is the same as in the solvolysis of (*R*)-**1**. One can, therefore, conclude that the same achiral intermediates are responsible for the formation of alcohols **3** and **4** from both precursors **1** and **2**. As addition of 9.5 mM $LiClO_4$ had no noticeable effect on the time-dependent yields of **1**–**4** during

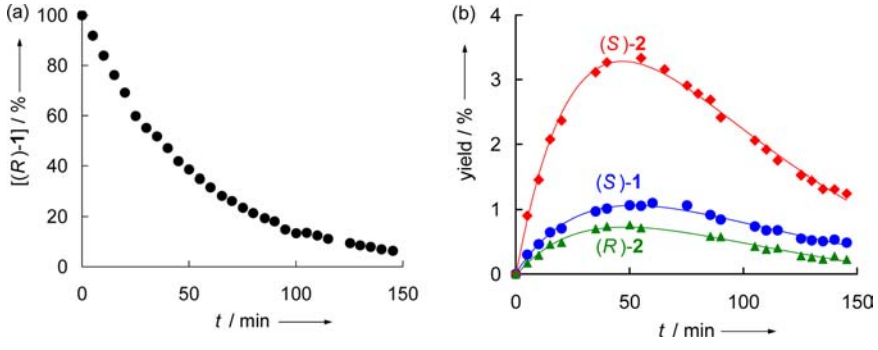

Figure 3. Time-dependent yields of (a) (*R*)-**1** and (b) (*S*)-**2**, (*S*)-**1**, and (*R*)-**2** during solvolysis of (*R*)-**1** (1.5 mM) in 60% aqueous acetone, 25 °C.

dx.doi.org/10.1021/ja308670g | J. Am. Chem. Soc. 2013, 135, 252–265

the solvolysis of (*R*)-**1** in 60% aqueous acetone (see pp S44–S46 of the Supporting Information), the participation of SSIPs cannot play a significant role (otherwise a special salt effect[30] would be expected). Therefore, alcohols **3** and **4** must be formed via the free 1-(4-chlorophenyl)-3-phenylallylium ions (**6**) or through ion pairs which interconvert more rapidly than they react with water. The preferred formation of **3** over **4** can be explained by the charge distribution in **6** and does not reflect the relative thermodynamic stabilities of **3** and **4** (a ratio of [**3**]/[**4**] = 0.88 was obtained by equilibration in the presence of *p*-toluenesulfonic acid; see p S57 of the Supporting Information for details). According to natural bond orbital (NBO) analysis (see p S96 of the Supporting Information for details), the positive charge is greater on the phenyl-substituted allyl terminus of the 1,3-diarylallyl cation, as phenyl stabilizes carbocations better than 4-chlorophenyl. These observations are consistent with results obtained by Easton et al. for other unsymmetrical allyl derivatives.[46] The stereospecificity of the allylic rearrangement of (*S*)-**2** in 60% aqueous acetone is also analogous to the previous case: (*R*)-**1** is the major isomerization product, followed by (*S*)-**1** and (*R*)-**2** (Figure S30).

Solvolysis of (R)-1 in 80% and 90% Aqueous Acetone. The rate of consumption of (*R*)-**1** in acetone–water mixtures decreases from 60% to 80% and 90% aqueous acetone (k_{rel} = 73, 7, and 1, respectively), as expected from the solvent ionizing power *Y*.[47] Figure 4 shows that the yield of rearranged esters increases considerably with decreasing water content in the solvent and that the sequence [(*S*)-**2**] > [(*S*)-**1**] > [(*R*)-**2**] does not change, which can be explained by decreasing dissociation abilities of the solvents (ε_r)[48] and increasing nucleophilicities of $^-$OPNB from 60% to 80% and 90% aqueous acetone (as observed for acetate anion[37]).

Solvolysis of (R)-1 in the Presence of External Nucleophiles. When the solvolysis of (*R*)-**1** in 60% aqueous acetone was performed in the presence of piperidine (54.2 mM), 40% of the allyl cations **6** were intercepted by the amine, leading to the formation of the regioisomeric (*E*)-1,3-diarylallylpiperidines in ca. 1:1 ratio (^{1}H NMR), and the total yield of the alcohols decreased to ca. 60%. Non-regioselective formation of 1,3-diarylallylpiperidines can be explained by diffusion-controlled reaction of piperidine with both allylic termini of the cation, which is in agreement with the prediction based on reactivity parameters of piperidine and **6**.[50] The same product ratio was found for the reaction of piperidine with the free cation **6** in dichloromethane (see p S6 of the Supporting Information for details).

In the presence of sodium azide (70.8 mM), allyl azide was the major product of the solvolysis reaction of (*R*)-**1** in 60% aqueous acetone, and the total yield of **3** and **4** was only about 3%. These observations show that the intermediates which give rise to the formation of **3** and **4** can be intercepted almost quantitatively by external nucleophiles, which is in agreement with the hypothesis that these intermediates are free 1,3-diarylallyl cations **6**. On the other hand, the various isomerization pathways of (*R*)-**1** were differently affected by external nucleophiles. The yield of (*S*)-**2**, which reached a maximum of 3.2% in the absence of nucleophiles, was only slightly reduced to 2.6% in the presence of piperidine (54.2 mM), and to 2.4% in the presence of NaN_3 (70.8 mM). In contrast, the same concentrations of NaN_3 reduced the formation of (*S*)-**1** by a factor of 2.2 (Figure 5) and [(*R*)-**2**] below the detection limit (not shown in Figure 5; see Figure S24a). An analogous situation was observed for the solvolysis of (*S*)-**2** in the presence of 76.6 mM NaN_3 (Figure S33).

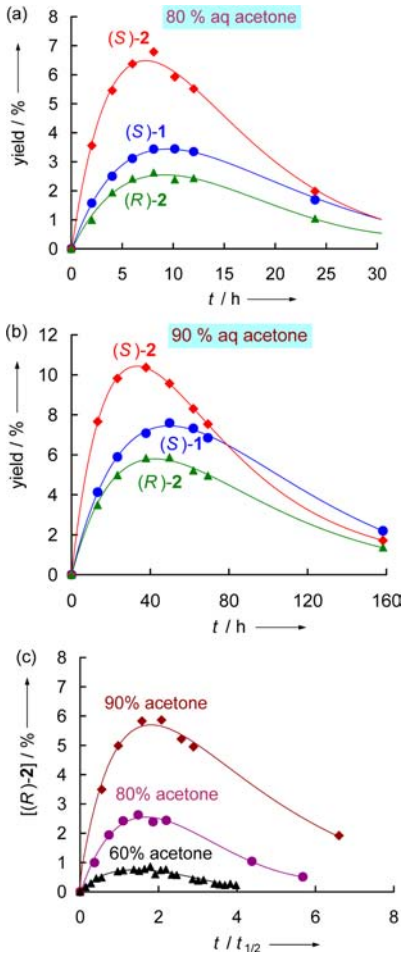

Figure 4. Time-dependent yields of (*S*)-**2**, (*S*)-**1**, and (*R*)-**2** during solvolysis of (*R*)-**1** in (a) 80% aqueous acetone ($[(R)\text{-}\mathbf{1}]_0$ = 0.77 mM) and (b) 90% aqueous acetone ($[(R)\text{-}\mathbf{1}]_0$ = 0.68 mM) as well as (c) yields of (*R*)-**2** during solvolyses of (*R*)-**1** in 60% ($[(R)\text{-}\mathbf{1}]_0$ = 1.5 mM), 80% ($[(R)\text{-}\mathbf{1}]_0$ = 0.77 mM), and 90% ($[(R)\text{-}\mathbf{1}]_0$ = 0.68 mM) aqueous acetone.[49]

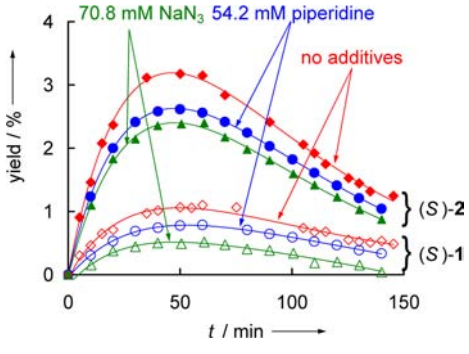

Figure 5. Time-dependent yields of (*S*)-**2** (filled points) and (*S*)-**1** (open points) generated during solvolysis of (*R*)-**1** (0.80–1.5 mM) without and with added nucleophiles (60% aqueous acetone, 25 °C).

Addition of chloride ions reduced the yields of the rearranged diarylallyl 4-nitrobenzoates (*S*)-**1**, (*S*)-**2**, and (*R*)-**2** to similar extents (Figures S19 and S22). Since the 1,3-diarylallyl chlorides formed by trapping of the free cation **6** by

dx.doi.org/10.1021/ja308670g | J. Am. Chem. Soc. 2013, 135, 252–265

Cl^- undergo fast dissociation to regenerate **6**, the yields of the hydrolysis products **3** and **4** were not affected, however.

Solvolysis of (R)-1 in the Presence of Tetrabutylammonium 4-Nitrobenzoate (Common Ion Return). Small amounts of Bu_4NOPNB (4.8 mM) reduced the rate of consumption of (*R*)-**1** in 60% aqueous acetone by only 7% (Figure S9a), while the yields of (*S*)-**2** (Figure 6a), (*R*)-**2** (Figure 6b), and (*S*)-**1** (Figure 6c) increased by factors of 1.3, 2.5, and 2, respectively. When a high concentration of Bu_4NOPNB (52.5 mM) was present, the consumption of (*R*)-**1** became significantly slower (factor of 0.65, common ion rate depression), and the yield of (*S*)-**2** increased by a factor of 2.5 (Figure 6a), while the yields of (*R*)-**2** and (*S*)-**1** were approximately 8 (Figure 6b) and 6.5 (Figure 6c) times higher than those in the absence of 4-nitrobenzoate. In summary, Bu_4NOPNB additives increased the yields of (*R*)-**2** and (*S*)-**1** by a significantly higher factor than the yield of (*S*)-**2**.

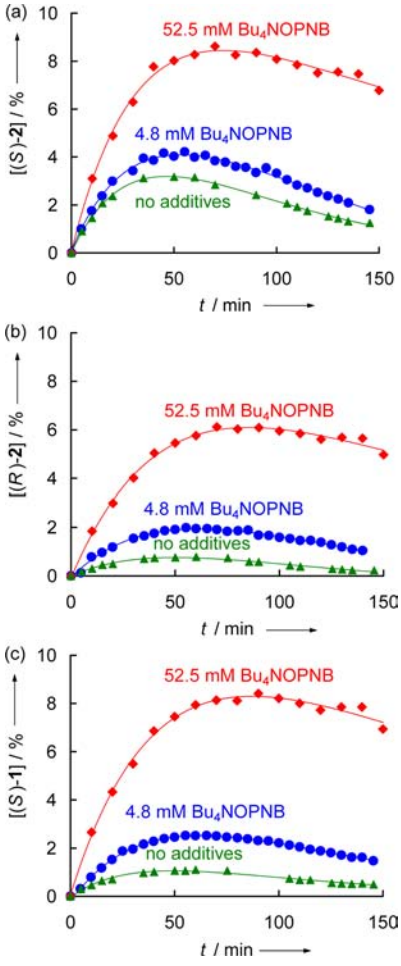

Figure 6. Time-dependent yields of (a) (*S*)-**2**, (b) (*R*)-**2**, and (c) (*S*)-**1** generated during solvolysis of (*R*)-**1** (0.78−1.5 mM) in the presence of various amounts of Bu_4NOPNB (60% aqueous acetone, 25 °C).

Reaction of the Diarylallyl Cation 6 with Water in Aqueous Acetone. In order to put the trapping reactions of the intermediate diarylallyl cation **6** on an absolute scale, we directly measured the rate of consumption of laser flash photolytically generated **6** in 60% aqueous acetone. As acetone has strong absorption in the UV region, excitation at $\lambda < 310$ nm, as used in routine laser flash experiments,[42] was not possible. For that reason, a modified procedure[51] was applied using a mixture of SuperDMAP-derived salts **8** and **9** which can be excited at 355 nm (Scheme 4).

The reaction with water was followed spectrophotometrically at the absorption maximum of **6** (510 nm), and the rate constant for the reaction of **6** with water (k_{solv}= 1.34 × 10^7 s^{-1}) was obtained by fitting the time-dependent absorbance to the monoexponential function $A_t = A_0\, e^{-k_{solv}t} + C$. As the k_{solv} values obtained at three different precursor concentrations agreed within the experimental error range (±5%), the influence of the photo-leaving group or impurities, which might be present in the stock solution of the precursors, on the reaction kinetics can be excluded.

DISCUSSION

We now develop a mechanistic scheme that accounts for the experimental findings. The observation that (*S*)-**2** is the preferred rearrangement product during the solvolysis of (*R*)-**1** and, vice versa, (*R*)-**1** is the preferred rearrangement product during the solvolysis of (*S*)-**2** indicates that there is a special pathway interconnecting these two isomers. Can it be a 1,3-sigmatropic rearrangement that avoids the intermediate formation of allyl cations?

If this were the case, then decreasing solvent ionizing power,[47] i.e., changing from 60% aqueous acetone to 80% and 90% aqueous acetone, should decrease the yields of esters formed by ionic pathways relative to those generated by a sigmatropic rearrangement. Comparison of Figures 3b, 4a, and 4b shows that the ratio [(*S*)-**2**]/([(*S*)-**1**] + [(*R*)-**2**]) decreases even in less ionizing solvents, which clearly rules out a sigmatropic rearrangement of (*R*)-**1** into (*S*)-**2** and vice versa.

In line with Goering's observations for cyclic allyl cations, we therefore conclude that the preferred isomerization (*R*)-**1**→(*S*)-**2** proceeds via suprafacial migration of the carboxylate anion at the CIP stage.

Figure 5 shows that the addition of NaN_3 (70.8 mM) and piperidine (54.2 mM) reduces the yield of (*S*)-**2** to a much smaller extent (factors of 1.3 and 1.2, respectively) than that of (*S*)-**1** (factors of 2.2 and 1.5, respectively). The behavior of (*R*)-**2** is similar to that of (*S*)-**1** (Figure S24a). Cl^- ions exert similar effects (Figure S19a). Vice versa, the addition of 4.8 mM Bu_4NOPNB increases the maximum concentration of (*S*)-**2** by a factor of only 1.3 (Figure 6a), while the yields of (*R*)-**2** (Figure 6b) and (*S*)-**1** (Figure 6c) grow by factors of 2−2.5.

Scheme 4. Laser Flash Photolytic Generation of the 1,3-Diarylallyl Cation 6 in 60% Aqueous Acetone

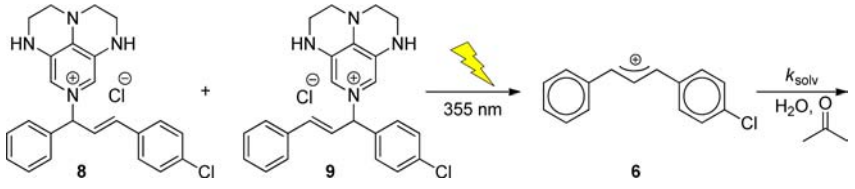

dx.doi.org/10.1021/ja308670g | J. Am. Chem. Soc. 2013, 135, 252−265

These observations indicate that the isomerizations of the 4-nitrobenzoates (*R*,*S*)-**1** as well as of (*R*,*S*)-**2** proceed via two different pathways: one that is affected by external nucleophiles (including common ions, external return[52]), and one that is not affected by external nucleophiles (internal return). The preferred rearrangement of (*R*)-**1** into (*S*)-**2**, where the LG stays on the same face of the allyl cation, is rationalized by internal return, which is not 100% stereospecific, however, because part of (*S*)-**1** and (*R*)-**2** must also arise from internal return. The latter conclusion is derived from the observation that 70.8 mM NaN_3 reduces the yield of (*S*)-**1** at the maximum of the curve in Figure 5 to 45% of the value observed in the absence of additives, while the same concentration of azide ions reduces the total yield of the hydrolysis products **3** and **4** from 100% to 3%. If (*S*)-**1** were exclusively formed through external return, i.e., by trapping of **6** by $^-$OPNB, then the yield of (*S*)-**1** should be reduced by a factor of 30, as observed for the yields of alcohols **3** and **4**.

The isomer (*R*)-**2** shows behavior similar to that of (*S*)-**1**, but a precise evaluation of the small quantities of (*R*)-**2** is problematic because of the broadness of the HPLC peak of this isomer (Figure 1). Complementary observations were made for the solvolysis of (*S*)-**2** (see pp S50 and S51 of the Supporting Information for details). We therefore conclude that the rearrangements through ion pairs proceed not only via suprafacial migration of carboxylate anion but also via migration of the carboxylate anion to the other face of the allyl cation without dissociation to the free ions.

Table 2 shows that the time-dependent difference $\Delta_t = [(S)\text{-}2]_t - [(R)\text{-}2]_t$ is independent (within experimental error) of

Table 2. Difference $\Delta_t = [(S)\text{-}2]_t - [(R)\text{-}2]_t$ at Certain Reaction Times during Solvolysis of (*R*)-1 in the Presence of Various Additives (60% Aqueous Acetone, 25 °C)

	Δ_t / %				
additive	at 10 min	at 20 min	at 40 min	at 50 min	at 60 min
none	1.2	1.9	2.5	2.4	2.4
4.8 mM Bu_4NOPNB	1.0	1.8	2.1	2.1	2.0
52.5 mM Bu_4NOPNB	1.3	1.9	2.7	2.6	2.5
54.2 mM piperidine	1.1	1.8	2.5	2.6	2.4
70.8 mM NaN_3	1.1	1.8	2.4	2.4	2.4

the nature and concentration of the external nucleophile. If external nucleophiles were able to attack the CIPs, the value of Δ_t could not be nucleophile-independent. One can, therefore, conclude that the CIPs generated in this system are inert to any additive used in the present work, including strong nucleophiles such as N_3^-.

These observations exclude the solvolysis mechanism proposed by Dvorko et al.,[53] who assumed that the azide anion generally attacks the CIPs rather than SSIPs or CSIPs (cavity-separated ion pairs), which are proposed by Dvorko to be intermediates on the way from CIP to SSIP in Scheme 2.

As discussed above, the formation of (*S*)-**1** and (*R*)-**2** from (*R*)-**1** can be suppressed by strong nucleophiles, such as NaN_3, by more than 50%. Internal return, therefore, is not the major pathway for the formation of these isomers, and external return[52] must be their main source, particularly when the reactions are carried out in the presence of Bu_4NOPNB. A similar situation is observed when (*S*)-**2** is used as a substrate, where internal return favors the formation of (*R*)-**1** (suprafacial migration product). Table 3 shows that the ratio [(*S*)-**1**]/[(*R*)-**2**] obtained by solvolysis of either (*R*)-**1** or (*S*)-**2** is the same within experimental accuracy, indicating common intermediates from both precursors. This observation definitely excludes that the rearrangements (*R*)-**1**→(*S*)-**1** and (*S*)-**2**→(*R*)-**2** are preferred over the rearrangements (*R*)-**1**→(*R*)-**2** and (*S*)-**2**→(*S*)-**1**, respectively. In other words, when the LG migrates to the other face of the allyl cation, it has no preference for the carbon from which it departs. The observation that the ratio [(*S*)-**1**]/[(*R*)-**2**] is comparable to the ratio of the hydrolysis products ([**3**]/[**4**] = 1.5), supports the suggestion that external return of $^-$OPNB (the major source of (*S*)-**1** and (*R*)-**2** in the presence of Bu_4NOPNB) and hydrolysis proceed via the same key intermediates, i.e., the free 1,3-diarylallyl cations **6**.

Table 3. Ratios [(*S*)-1]/[(*R*)-2] at Certain Reaction Times during Solvolysis of (*R*)-1 and (*S*)-2 in the Presence of Various Additives (60% Aqueous Acetone, 25 °C)

	[(*S*)-**1**]/[(*R*)-**2**]	
substrate, additive	at 50 min	at 60 min
(*R*)-**1**, no additive	1.40	1.41
(*R*)-**1**, 4.8 mM Bu_4NOPNB	1.28	1.29
(*R*)-**1**, 52.5 mM Bu_4NOPNB	1.37	1.38
(*S*)-**2**, no additive	1.35	1.50

A summary of these observations is presented in Scheme 5. The ionization step (k_1 starting from **1** or k'_1 starting from **2**) provides contact ion pairs ((*R*)-CIP_1, (*S*)-CIP_1, (*R*)-CIP_2, (*S*)-CIP_2) which retain the stereochemical and regiochemical information of the covalent substrates; i.e., the 4-nitrobenzoate anion is still on the same face of the carbocationic plane, close to the carbon to which it was covalently bound in the starting material. While these unsymmetrical structures of the ion pairs are in agreement with previous suggestions by Goering[54] and Thibblin,[55] the distinction of four different ion pairs is in line with, but not inevitably required by, our experimental data. Instead of assuming the rapidly equilibrating pairs (*R*)-$CIP_1 \rightleftharpoons$(*S*)-CIP_2 and (*S*)-$CIP_1 \rightleftharpoons$(*R*)-CIP_2, one might also assume that the same chiral ion pair is formed from (*R*)-**1** and (*S*)-**2**, which is enantiomeric to that generated from (*S*)-**1** and (*R*)-**2**. The latter alternative is kinetically equivalent to the mechanism in Scheme 5 (four different CIPs) with $k_r = k'_r = \infty$. According to Scheme 5, the unsymmetrical CIPs can undergo recombination (k_{-1} and k'_{-1}), suprafacial migration (k_r and k'_r), inversion (k_i, k'_i, the anion migrates to the opposite face of the allyl cation), and dissociation with formation of free cations **6** (k_2, k'_2). The free cations can reassociate with 4-nitrobenzoate anions, regenerating the CIPs with the second-order rate constants k_{-2} and k'_{-2}, or react with other nucleophiles (represented in Scheme 5 with the effective first-order rate constant k_{Nu}, which corresponds to the sum of reactions with all external nucleophiles and water) to produce the racemic products **3**, **4**, **7**, and **7′**. As alcohols **3** and **4** are formed as racemates, nucleophilic trapping of the chiral CIPs can be excluded in Scheme 5. Trapping of ion pairs by external nucleophiles must be taken into account, however, when ion pairs of less stabilized carbocations are involved.[56]

The gross rate constant of the diffusional encounter of **6** with $^-$OPNB (k_{diff}^{OPNB}) is expressed by eq 1:

$$k_{OPNB}^{diff} = 2(k_{-2} + k'_{-2}) \quad (1)$$

dx.doi.org/10.1021/ja308670g | J. Am. Chem. Soc. 2013, 135, 252−265

Scheme 5. Mechanism for the Solvolysis of Allyl 4-Nitrobenzoates 1 and 2[a]

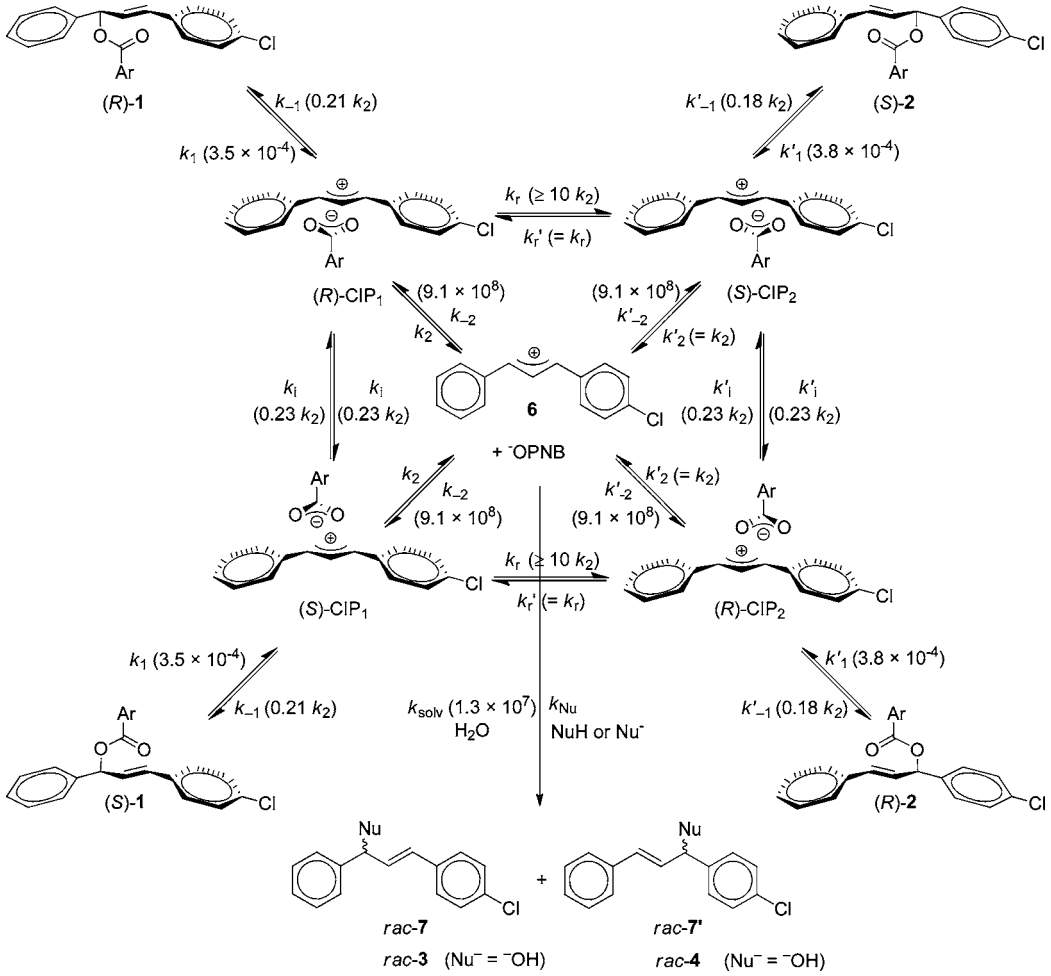

[a]The rate constants shown in parentheses result from the fit described below. All first-order rate constants as well as the pseudo-first-order rate constant k_{solv} are given in s^{-1} and correspond to 60% aqueous acetone, 25 °C. Second-order rate constants k_{-2} and k'_{-2} are given in $M^{-1}\ s^{-1}$.

The factor of 2 implies that the encounter of **6** with $^{-}$OPNB is split into two equal pathways leading to the enantiomeric ion pairs.

The interconversions depicted in Scheme 5 can be described by the rate laws in eqs 2−10.

$$\frac{d[(R)\text{-}\mathbf{1}]}{dt} = -k_1[(R)\text{-}\mathbf{1}] + k_{-1}[(R)\text{-ClP}_1] \quad (2)$$

$$\frac{d[(S)\text{-}\mathbf{1}]}{dt} = -k_1[(S)\text{-}\mathbf{1}] + k_{-1}[(S)\text{-ClP}_1] \quad (3)$$

$$\frac{d[(R)\text{-}\mathbf{2}]}{dt} = -k'_1[(R)\text{-}\mathbf{2}] + k'_{-1}[(R)\text{-ClP}_2] \quad (4)$$

$$\frac{d[(S)\text{-}\mathbf{2}]}{dt} = -k'_1[(S)\text{-}\mathbf{2}] + k'_{-1}[(S)\text{-ClP}_2] \quad (5)$$

$$\frac{d[(R)\text{-ClP}_1]}{dt} = k_1[(R)\text{-}\mathbf{1}] + k'_r[(S)\text{-ClP}_2] + k_i[(S)\text{-ClP}_1] + k_{-2}[\mathbf{6}][^{-}\text{OPNB}] - (k_{-1} + k_r + k_i + k_2)[(R)\text{-ClP}_1] \quad (6)$$

$$\frac{d[(S)\text{-ClP}_1]}{dt} = k_1[(S)\text{-}\mathbf{1}] + k'_r[(R)\text{-ClP}_2] + k_i[(R)\text{-ClP}_1] + k_{-2}[\mathbf{6}][^{-}\text{OPNB}] - (k_{-1} + k_r + k_i + k_2)[(S)\text{-ClP}_1] \quad (7)$$

$$\frac{d[(R)\text{-ClP}_2]}{dt} = k'_1[(R)\text{-}\mathbf{2}] + k_r[(S)\text{-ClP}_1] + k'_i[(S)\text{-ClP}_2] + k'_{-2}[\mathbf{6}][^{-}\text{OPNB}] - (k'_{-1} + k'_r + k'_i + k'_2)[(R)\text{-ClP}_2] \quad (8)$$

$$\frac{d[(S)\text{-ClP}_2]}{dt} = k'_1[(S)\text{-}\mathbf{2}] + k_r[(R)\text{-ClP}_1] + k'_i[(R)\text{-ClP}_2] + k'_{-2}[\mathbf{6}][^{-}\text{OPNB}] - (k'_{-1} + k'_r + k'_i + k'_2)[(S)\text{-ClP}_2] \quad (9)$$

$$\frac{d[\mathbf{6}]}{dt} = k_2[(R)\text{-ClP}_1] + k_2[(S)\text{-ClP}_1] + k'_2[(R)\text{-ClP}_2] + k'_2[(S)\text{-ClP}_2] - (2k_{-2}[^{-}\text{OPNB}] + 2k'_{-2}[^{-}\text{OPNB}] + k_{Nu})[\mathbf{6}] \quad (10)$$

dx.doi.org/10.1021/ja308670g | J. Am. Chem. Soc. 2013, 135, 252−265

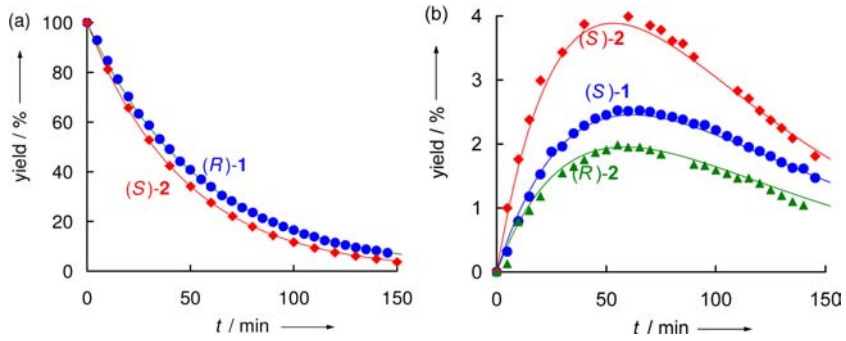

Figure 7. Calculated (solid lines) and experimental time-dependent yields of (a) (*R*)-**1** (0.80 mM) and (*S*)-**2** (0.79 mM) during their solvolysis in 60% aqueous acetone in the presence of 4.8 mM Bu_4NOPNB and 76.6 mM NaN_3, respectively; and (b) of (*S*)-**1**, (*S*)-**2**, and (*R*)-**2** during solvolysis of (*R*)-**1** (0.80 mM) in 60% aqueous acetone in the presence of 4.8 mM Bu_4NOPNB, 25 °C.

The solution of the system of linear ordinary differential eqs 2−10 provides the calculated values for the time-dependent yields of (*R*)-**1**, (*S*)-**1**, (*R*)-**2**, and (*S*)-**2** for a given set of parameters (k_1, k'_1, k_{-1}, k'_{-1}, k_r, k_i, k'_r, k'_i, k_2, k'_2, $k_{-2}[^-OPNB]$, $k'_{-2}[^-OPNB]$, k_{Nu}).[57] In order to determine the individual rate constants shown in Scheme 5, we have simulated the time-dependent yields of the four isomeric esters (*R*)-**1**, (*S*)-**1**, (*R*)-**2**, and (*S*)-**2** during the solvolysis in 60% aqueous acetone of (i) (*R*)-**1** (0.80 mM) in the presence of 70.8 mM NaN_3, which provides reliable data for internal return because external return of ^-OPNB is almost completely suppressed ($k_{-2}[^-OPNB] \ll k_{Nu} = k_{N3}[N_3^-] + k_{solv}$); (ii) (*S*)-**2** (0.79 mM) in the presence of 76.6 mM NaN_3; and (iii) (*R*)-**1** (0.80 mM) in the presence of 4.8 mM Bu_4NOPNB (to keep $k_{-2}[^-OPNB]$ and $k'_{-2}[^-OPNB]$ constant during the reaction, which provides the reliable data for external return).

The directly measured rate constant of the reaction of **6** with water in 60% aqueous acetone ($k_{solv} = 1.34 \times 10^7$ s^{-1}) and the second-order rate constant k_{N3} (6.1×10^9 M^{-1} s^{-1}), which was derived from k_{solv} and the allyl azide/allyl alcohol ratio, were introduced as fixed quantities.

As the free energies of the ion pairs CIP_1 and CIP_2 are closely similar, the corresponding rate constants for diffusion and ion pair reorganization were set equal, i.e., $k'_2 = k_2$, $k'_{-2} = k_{-2}$, $k'_r = k_r$, and $k'_i = k_i$. The small errors introduced by these assumptions are compensated by the relative magnitudes of the recombination rate constants k'_{-1}/k_{-1}.

Minimization of the sum of squared deviations (SSD) between calculated and experimental time-dependent yields of all isomeric esters (*R,S*)-**1** and (*R,S*)-**2** yielded the values of the rate constants which fit the experiments most correctly.

As shown in Table SN1 of the Supporting Information, $k_2 = k'_2$ was arbitrarily set at values between 10^8 and 10^{11} s^{-1}, while the remaining parameters were optimized. The last column of Table SN1 shows that equally good fits between calculated and experimental yields were obtained for the different values of $k_2 = k'_2$. While k_1, k'_1, k_{-2}, and k'_{-2} were found to be independent (±4%) of the choice of k_2 in the specified range, k_{-1}, k'_{-1}, and $k_i = k'_i$ were found to be directly proportional to k_2 (Figures SN1−SN8), which allowed us to express these rate constants as multiples of k_2 in Scheme 5. For a fixed value of $k_2 = k'_2 = 2 \times 10^{10}$ s^{-1}, comparable SSDs were obtained for different values of k_r as long as they were greater than $10k_2$, and the values of k_{-1}, k'_{-1}, $k_i = k'_i$ changed insignificantly (<7%) when $k_r = k'_r$ was varied from $10k_2$ to $500k_2$ (Figures SN9−SN15). As a consequence, each value of k_2 entails certain values (±7%) of k_{-1}, k'_{-1}, $k_i = k'_i$ and lower limits for $k_r = k'_r$. The same results were obtained when the steady-state approximation was applied to (*R*)-CIP_1, (*S*)-CIP_1, (*R*)-CIP_2, (*S*)-CIP_2, and **6** (Figures SN1a−SN8a). The resulting absolute and relative rate constants are presented in Scheme 5.

The good agreement between calculated and experimental time-dependent yields (Figure 7 and Figures SN18 and SN19) demonstrates that the solvolyses of **1** and **2** can be adequately described by the mechanism presented in Scheme 5.

According to Scheme 5, the slowest step of the solvolysis is the initial ionization leading to the CIPs ($k_1 = 3.5 \times 10^{-4}$ s^{-1}, $k'_1 = 3.8 \times 10^{-4}$ s^{-1}). Suprafacial migration of the 4-nitrobenzoate anion ($k_r = k'_r > 10k_2$) is the most likely transformation of the CIP, followed by dissociation ($k_2 = k'_2$) and, finally, inversion ($k_i = k'_i = 0.23k_2$) and ion pair collapse ($k_{-1} = 0.21k_2$, $k'_{-1} = 0.18k_2$), which have almost equal rates. This sequence explains the partial stereospecificity of internal return, i.e., the fact that (*S*)-**2** is the major product among the rearranged esters during solvolysis of (*R*)-**1** and vice versa.

Because of the availability of the directly measured rate constant k_{solv} for the reaction of **6** with water (in aqueous acetone), our experiments provide an accurate value for the rate constant of the diffusional process generating ion pairs from the free ions **6** ($k_{-2} = k'_{-2}$). On the other hand, the rate constants for the diffusional separation of the ion pairs ($k_2 = k'_2$) cannot be derived directly from the experimental data. As values of $10^8 < k_2/s^{-1} < 10^{11}$ give equally good fits, the value of $k_2 \approx 1.6 \times 10^{10}$ s^{-1}, which was proposed by Richard and Jencks[35] and is mostly used in the literature, appears to be a good choice also for this system.

From the value of $k_{-2} = k'_{-2} = 9.1 \times 10^8$ M^{-1} s^{-1}, one can calculate the second-order rate constant of diffusional migration of 4-nitrobenzoate anion to the free cation **6** using eq 1 ($k_{diff}^{OPNB} = 4k_{-2} = 3.6 \times 10^9$ M^{-1} s^{-1}), which is similar to the value of 1.5×10^9 M^{-1} s^{-1} reported by Tsuji, Richard, and co-workers for the diffusion of carboxylate anions to the 1-(4-methylphenyl)-ethyl cation in 50% v/v TFE−water mixture.[36a]

Earlier analyses, which were based on titrimetric, polarimetric, and ^{18}O-exchange rate constants, left the question open whether solvolysis and internal return are two independent processes involving different types of ion pairs.[33] As simulations based on Scheme 5 accurately describe the distribution of the products generated by internal and external return, it is now clear that solvolysis and internal return can be explained by the same intermediates.

dx.doi.org/10.1021/ja308670g | J. Am. Chem. Soc. 2013, 135, 252−265

A COMPREHENSIVE VIEW ON SOLVOLYSES OF ALLYL CARBOXYLATES

The kinetic and stereochemical investigations of the solvolyses of the enantiopure allyl carboxylates (*R*)-**1** and (*S*)-**2** provided detailed information on relative and absolute rates of the individual steps for the system described in Scheme 5. Can one use these results to derive a general scheme of solvolyses of allyl carboxylates?

In previous work,[44] we have determined the electrophilicity parameters *E* of the symmetrical 1,3-diarylallyl cations X-**10**, which are listed in Table 4. According to eq 11, the

$$\log k(20\ ^\circ\mathrm{C}) = s_N(E + N) \tag{11}$$

electrophilicity parameters *E* can be combined with the solvent-dependent nucleophile-specific parameters *N* and s_N to calculate second-order rate constants for the reactions of carbocations with neutral and anionic nucleophiles[39] as well as the first-order rate constants for the reactions of carbocations with the solvents.[38]

As the 1,3-diphenylallyl cation H-**10** and its dichloro-substituted analogue Cl-**10** have almost the same values of *E*, the same electrophilicity ($E = 2.70$) can also be assumed for the monochlorinated system **6**.

Table 4. Symmetrical 1,3-Diarylallyl Cations X-10 and Their Electrophilicity Parameters *E*[44]

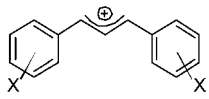

X - **10**

X-**10**	X	*E*
F_2-**10**	*m*,*m*-F_2	6.11
F-**10**	*m*-F	4.15
Br-**10**	*p*-Br	2.85
Cl-**10**	*p*-Cl	2.69
H-**10**	H	2.70
Me-**10**	*p*-Me	1.23
MeO-**10**	*p*-MeO	−1.45
Me_2N-**10**	*p*-Me_2N	−7.50

Rates of Reactions of the Allyl Cations 10 with Aqueous Acetone. Investigations of the nucleophilic reactivities of solvents have shown that acetonitrile/water mixtures with 20% to 90% content of water (v/v) react with equal rates with benzhydrylium ions,[38] in accordance with earlier reports by McClelland.[58] The same relationship seems to hold also for acetone/water mixtures, as 90% ($N = 5.70$, $s_N = 0.85$) and 80% aqueous acetone ($N = 5.77$, $s_N = 0.87$) were reported to react with similar rates.[59] Accordingly, the first-order rate constant for the reaction of **6** ($E = 2.70$) with 80% aqueous acetone calculated by eq 11 ($2.3 \times 10^7\ s^{-1}$) agrees well with the directly measured rate constant for the reaction of **6** with 60% aqueous acetone ($1.34 \times 10^7\ s^{-1}$, see above). Equation 11 can thus be employed also to calculate the rate constants for the reactions of **10** with aqueous acetone.

It should be noted that the agreement within a factor of 2 between the calculated and experimental rate constant for the reaction of **6** with aqueous acetone cannot a priori be expected, because deviations up to factors of 10−100 have to be tolerated for predictions of absolute rate constants by eq 11, which covers a reactivity range of 40 orders of magnitude with only three parameters.[41,60] On the other hand, eq 11 allows one to predict relative reactivities within reaction series, e.g., the relative reaction rates of X-**10**,[44] with an accuracy better than factor of 2.[43,60]

Rates of Reactions of the Allyl Cations 10 with the 4-Nitrobenzoate Anion. In order to apply eq 11, let us first derive the nucleophilicity parameter *N* for the 4-nitrobenzoate anion ($^-$OPNB) in 60% aqueous acetone. At low concentrations of the substrates, as they are usually employed in solvolysis experiments, the concentration of ion pairs (corresponding to encounter complexes in ion−molecule or molecule−molecule reactions) is small compared with the concentrations of the nonpaired reactants, and the rate constant for the recombination of **6** with $^-$OPNB to the covalent products **1** and **2** is given by eq 12, which expresses the rate

$$k_{rec} = 2k_{-2}\frac{k_{-1}}{k_{-1} + k_2} + 2k'_{-2}\frac{k'_{-1}}{k'_{-1} + k'_2} \tag{12}$$

constants for ion recombination k_{rec} by multiplying the constant of the diffusional association (k_{-2}) with the partitioning factor (forward reaction, k_{-1}, divided by the sum of forward and backward reactions, $k_{-1} + k_2$) and the corresponding term for attack at the other allyl terminus. Substitution of k_{-1}, k'_{-1}, k_{-2}, and k'_{-2} by the absolute values or multiples of k_2 presented in Scheme 5 yields $k_{rec} = 5.91 \times 10^8\ M^{-1}\ s^{-1}$ for the reaction of **6** with $^-$OPNB in 60% aqueous acetone. As $k_{rec} > 10^8\ M^{-1}\ s^{-1}$, i.e., beyond the range which is covered by eq 11, k_{rec} cannot be directly substituted in eq 11 to calculate *N*.

For the sake of simplicity, let us adjust eq 12 to symmetrically substituted allyl cations, e.g., **10**. For $k'_{-1} = k_{-1}$, $k'_2 = k_2$, and $k'_{-2} = k_{-2}$, eq 12 simplifies to eq 13:

$$k_{rec} = 4k_{-2}\frac{k_{-1}}{k_{-1} + k_2} \tag{13}$$

In activation-controlled reactions of **10** with $^-$OPNB, diffusional separation is much faster than the formation of the covalent esters ($k_2 \gg k_{-1}$), which reduces eq 13 to eq 14:

$$k_{rec} = 4k_{-2}\frac{k_{-1}}{k_2} \tag{14}$$

It should be noted that eqs 13 and 14 correspond to the typical treatment of diffusion- and activation-controlled reactions described in standard textbooks.[61]

In order to apply the linear free energy relationship (eq 11) also to reactions which are affected by diffusion rates ($k > 10^8\ M^{-1}\ s^{-1}$), one has to multiply the rate constants calculated by eq 11 (which refer to activation-controlled reactions) with the correction factor *f* (eq 15), which is obtained by dividing eq 13 by eq 14:

$$f = \frac{k_2}{k_2 + k_{-1}} \tag{15}$$

For $k_{-1} = 0.193k_2$ (average of k_{-1} and k'_{-1}, Scheme 5),[62] one obtains $f = 0.84$. Division of the experimental rate constant for the reaction of **6** with $^-$OPNB ($5.91 \times 10^8\ M^{-1}\ s^{-1}$) by $f = 0.84$ leads to $7.04 \times 10^8\ M^{-1}\ s^{-1}$, which can be substituted into eq 11 to derive *N* ($^-$OPNB) = 9.94, using *E* (**6**) = 2.70 and $s_N = 0.7$, the typical sensitivity parameter for carboxylate anions in aqueous and polar organic solvents.[37] The *N* and s_N parameters

dx.doi.org/10.1021/ja308670g | J. Am. Chem. Soc. 2013, 135, 252−265

for $^{-}$OPNB can now be combined with the E values of X-**10** (Table 4) to calculate the rate constants for the reactions of X-**10** with 4-nitrobenzoate anion in 60% aqueous acetone.

Probabilities of Internal and External Return. Internal return occurs when the value of k_{-1} is comparable to or greater than the rate constant of diffusional separation of the ion pairs (k_2). Its probability is given by eq 16:

$$p_{IR} = \frac{k_{-1}}{k_{-1} + k_2} \times 100\% \quad (16)$$

From eqs 14 and 11 one gets eq 17, which allows k_{-1} to be expressed as a function of E (eq 18):

$$s_N(E + N) = \log 4k_{-2} + \log \frac{k_{-1}}{k_2} \quad (17)$$

$$\log k_{-1} = s_N(E + N) + \log k_2 - \log 4k_{-2} \quad (18)$$

For the sake of simplicity, let us assume that the linear dependence of log k_{-1}/k_2 on E, which is expressed by eqs 17 and 18, also holds for reactions beyond the activation-controlled region (i.e., for reactions where k_{-1} is comparable to k_2).[63] One then arrives at Figure 8, which illustrates the

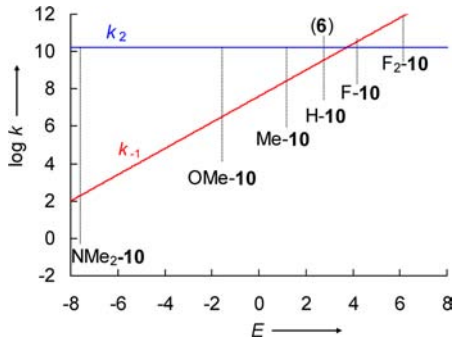

Figure 8. Relationship between internal return (k_{-1} vs k_2) and the electrophilicities E of the carbenium ions **10** during solvolyses of 1,3-diarylallyl 4-nitrobenzoates **10**-OPNB in 60% aqueous acetone.

increase of the rate of ion pair collapse (k_{-1}, from eq 18) with increasing electrophilicity E of the allyl cations X-**10** in comparison with the rate constant for diffusional separation (k_2), for which Richard's[35] estimate of 1.6×10^{10} s^{-1} is used.

One can see that the lines cross at $E \approx 4$; i.e., internal return becomes dominant for the highly electrophilic carbocations on the right of Figure 8. The k_{-1} graph is only slightly below the k_2 line for cation **6**, which reflects the participation of internal return expressed by the k_{-1}/k_2 ratio in Scheme 5. It should be emphasized that this analysis does not depend on the exact magnitude of k_2. According to eq 18, variation of k_2 would also affect k_{-1} and shift the crossing point of the two correlation lines in Figure 8 vertically, not horizontally; i.e., the nature of the carbocation (E value) where these lines cross would not be affected. The E value of the crossing point would move slightly, however, when the linear dependence of log k_{-1}/k_2 on E is not followed accurately in the diffusion-controlled range, as assumed above.

The probability of external return is given by the relative rates of the reactions of the free 1,3-diarylallyl cation **10** with 4-nitrobenzoate anion ($k_{rec}[^{-}OPNB]$) and the solvent (k_{solv}), as described by eq 19:

$$p_{ER} = \frac{k_{rec}[^{-}OPNB]}{k_{rec}[^{-}OPNB] + k_{solv}} \times 100\% \quad (19)$$

Figure 9 compares the pseudo-first-order rate constants for the reactions of the allyl cations **10** with the 4-nitrobenzoate

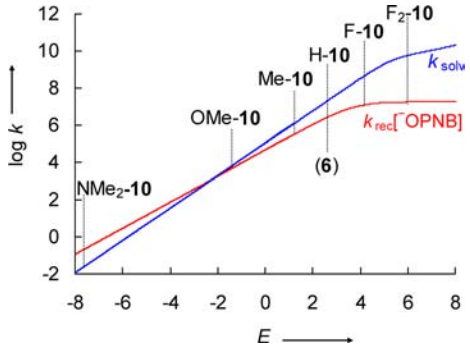

Figure 9. Relationship between external return (k_{rec} vs k_{solv}) and the electrophilicities E of the carbenium ions **10** during solvolyses of 1,3-diarylallyl 4-nitrobenzoates **10**-OPNB in 60% aqueous acetone for [$^{-}$OPNB] = 5 mM (25 °C).

anion in 60% aqueous acetone (at [$^{-}$OPNB] = 5 mM) and with the solvent calculated by eq 11. The curved part of the k_{rec} graph, which describes the approach to the diffusion limit, was obtained by multiplication of the rate constants calculated by eq 11 with the correction factor f of eq 15. The curvature of the correlation line for the solvent, which is irrelevant for the following discussion, is estimated from preliminary results in our group.[64]

As previously shown for solvolyses of benzhydryl and trityl derivatives,[41] external (common ion) return is faster than the reaction with solvent for highly stabilized carbocations, while highly reactive carbocations are so rapidly trapped by the solvent that the leaving group $^{-}$OPNB does not have a chance to compete because of its low concentration, even when the ion combination is diffusion-controlled.

The probabilities of internal return p_{IR} and external return p_{ER} can be calculated by eqs 16 and 19 and are plotted against E in Figure 10.[65]

According to Figure 10, solvolyses of 1,3-diarylallyl 4-nitrobenzoates in 60% aqueous acetone (at [$^{-}$OPNB] = 5 mM), which proceed via highly stabilized carbenium ions (E < 0, e.g., Me_2N-**10** or MeO-**10**), do not occur with internal return

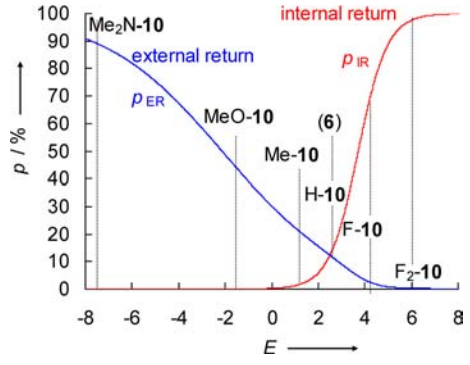

Figure 10. Dependencies of p_{IR} and p_{ER} for solvolyses of 1,3-diarylallyl 4-nitrobenzoates **10**-OPNB in 60% aqueous acetone (25 °C) on the E values of the cations **10** for [$^{-}$OPNB] = 5 mM.

dx.doi.org/10.1021/ja308670g | J. Am. Chem. Soc. 2013, 135, 252−265

because their diffusional escape from the ion pair cage is faster than ion pair collapse; allylic rearrangements of such systems should proceed completely non-stereospecific. Both external and internal return can be expected for the solvolyses of 4-nitrobenzoates derived from carbenium ions with $1 < E < 5$. While the extent of external and internal return is comparable for H-**10**-OPNB or **6**-OPNB (p_{IR} = 16%, p_{ER} = 11%), solvolysis via better stabilized allyl cations ($E < 2.7$) should give more external and those via less stabilized carbocations should give more internal return. Thus, 4-nitrobenzoates derived from carbenium ions with $E > 6$ (e.g., F_2-**10**-OPNB), should solvolyze without external and with a large degree of internal return, i.e., allylic rearrangements of unsymmetrical systems involving carbocations of such high electrophilicities can be expected to be highly stereospecific.

The far right part of Figure 10 has to be seen with some caveat, however, because it is based on the premise that solvent and 4-nitrobenzoate anions attack only at free cations and not at ion pairs, as demonstrated for the solvolysis of **6**-OPNB in this work. It is feasible, however, that in the case of highly electrophilic carbenium ions, direct solvent capture of the CIPs will occur, resulting in a decrease of the probability of internal return.

The scheme presented for 1,3-diarylallyl 4-nitrobenzoates in 60% aqueous acetone in Figure 10, i.e., increase of p_{IR} and decrease of p_{ER} with increasing electrophilicity E, should analogously hold for other leaving groups and solvents, though the positions of the curves and their shapes will change. Figure 11 illustrates the calculated curves for external and internal return for Br^- (N = 13.80, s_N = 0.60), a significantly stronger nucleophile[37,38] (though a weaker Lewis base) than $^-$OPNB, in 50% aqueous acetonitrile (N = 5.05, s_N = 0.89), a solvent of similar nucleophilicity as aqueous acetone.

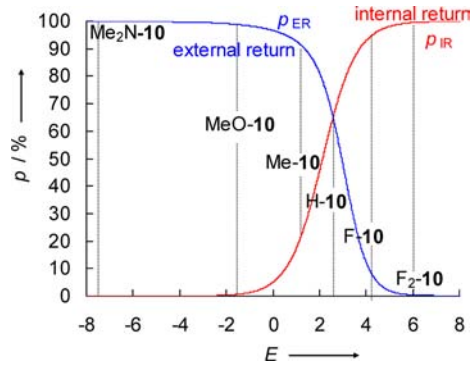

Figure 11. Estimated dependencies of p_{IR} and p_{ER} for solvolyses of 1,3-diarylallyl bromides **10**-Br in 50% aqueous acetonitrile (25 °C) on the E values of the cations **10** for [Br^-] = 5 mM.

One can see that the graph for internal return is similar to that in Figure 10, but shifted to less electrophilic carbocations, implying that internal return plays a greater role because of the higher nucleophilicity of Br^-. The graph for external return is almost the same in the right part of Figures 10 and 11 because both Br^- and $^-$OPNB undergo diffusion-controlled reactions with carbocations in this range and have comparable chances to compete with the nucleophilic attack by water. Moving to the left, i.e., to less electrophilic carbocations, leads to a much faster increase of external return in Figure 11, because now the better nucleophile Br^- can more efficiently compete with water than the weaker nucleophile $^-$OPNB. It should be noted, however, that the far left part of this graph is hypothetic. Though a fast reaction of Me_2N-**10** with Br^- will occur, the reverse reaction can be expected to be even faster, with the result that Me_2N-**10**$^+Br^-$ will be predominantly ionic in 50% aqueous acetonitrile.

Decrease of the water content in acetone/water and acetonitrile/water mixtures is known to increase the nucleophilicity parameters N of the commonly used anionic leaving groups,[39,66] resulting in an increase of k_{-1} according to eq 18 and consequently lead to an increase in p_{IR} (eq 16). As an increase of N will also increase k_{rec} (eq 11) and consequently p_{ER} (eq 19; the small decrease of k_{solv} in solvents with a lower content of water will shift p_{ER} in the same direction), also the probability of external return will grow. In line with this analysis, Figures 3 and 4 show an increase of the yields of all isomerization products ((*S*)-**1**, (*R*)-**2**, and (*S*)-**2**) generated during the solvolysis of (*R*)-**1** when the solvent was changed from 60% to 80% and 90% aqueous acetone. In the same way, one can rationalize Goering's observations that the ratio k_α/k_t (polarimetric rate constant/titrimetric rate constant) for the solvolyses of *cis*-5-methylcyclohex-2-enyl 2-carboxybenzoate,[26] *trans*-5-methylcyclohex-2-enyl 4-nitrobenzoate,[27b] and 1,3-dimethylallyl 4-nitrobenzoate[67] in aqueous acetone generally increased with decreasing water content because of the increasing nucleophilicities of the carboxylate ions. The enhancement of internal return with increasing electrophilicities of the carbenium ions is also in agreement with conclusions of Yabe and Kochi, which were derived from the rates of the recombinations of anthracenylium radical cation–trinitromethide ion pairs generated by laser-flash-induced electron transfer in the anthracene–tetranitromethane complexes.[32]

CONCLUSIONS

The time-dependent yields of the four isomeric esters (*R*,*S*)-**1** and (*R*,*S*)-**2** and the four isomeric alcohols (*R*,*S*)-**3** and (*R*,*S*)-**4** measured during the hydrolysis of enantiopure (*R*)-**1** and (*S*)-**2** in aqueous acetone in the presence and absence of external nucleophiles were combined with the measured rate constant for the reaction of the laser-flash photolytically generated allyl cation **6** with water in aqueous acetone in order to develop a complete mechanistic scheme for this solvolysis cascade. As depicted in Scheme 5, the slowest step is the initial ionization leading to the CIPs ($k_1 = 3.5 \times 10^{-4}$ s^{-1}, $k'_1 = 3.8 \times 10^{-4}$ s^{-1}). Suprafacial migration of the 4-nitrobenzoate anion ($k_r = k'_r > 10k_2$) is the most likely transformation of the CIP, followed by dissociation ($k_2 = k'_2$) and, finally, inversion ($k_i = k'_i = 0.23k_2$) and ion pair collapse ($k_{-1} = 0.21k_2$, $k'_{-1} = 0.18k_2$). This sequence explains the partial stereospecificity of internal return, i.e., the fact that (*S*)-**2** is the major product among the rearranged esters during solvolysis of (*R*)-**1** and vice versa. As simulations based on Scheme 5 accurately describe the distribution of the products generated by internal and external return, it is now clear that solvolysis and internal return can be explained by the same intermediates.

The results of this work were combined with previously determined electrophilicity parameters E for 1,3-diarylallyl cations X-**10** to analyze the role of internal and external return in solvolyses of 1,3-diarylallyl 4-nitrobenzoates. While the parent 1,3-diphenylallyl 4-nitrobenzoate (E = 2.7) is predicted to solvolyze with 16% internal and 11% external return,[65] the contribution of external return increases, and the contribution of internal return decreases with increasing stabilization (decreasing electrophilicity E) of the allyl cations (Figure 10).

dx.doi.org/10.1021/ja308670g | J. Am. Chem. Soc. 2013, 135, 252–265

The correlation eq 11, which calculates rate constants of the reactions of carbocations with nucleophiles from the electrophile-specific parameter E and the nucleophile-specific parameters N and s_N, can be used to estimate the role of internal and external return also for other substrates.

EXPERIMENTAL SECTION

Acetone (99.8%), hexane, and isopropanol (HPLC grade) were used as received. Doubly distilled water (impedance 18.2 Ω) was obtained from a water purification system. Tetrabutylammonium chloride and sodium azide were purchased and used without further purification. Tetrabutylammonium 4-nitrobenzoate and tetrabutylammonium benzoate were synthesized by using the procedure described in ref 37. Sharpless kinetic resolution followed by acylation was used for synthesis of optically active **1** and **2**. The absolute configuration of (*R*)-**1** was confirmed by X-ray diffraction analysis.[68] The precursors for laser-flash measurements, **8** and **9**, were generated in situ from the mixture of 1-(4-chlorophenyl)-3-phenylallyl and 3-(4-chlorophenyl)-1-phenylallyl chlorides (**11**) synthesized from **3** using the procedure from ref 69 and 1,2,3,4,5,6-hexahydro-1,3a,6,8-tetraazaphenalene (**12**) obtained as reported by David and co-workers.[70] Detailed descriptions of HPLC experiments, laser-flash kinetic measurements, and NMR product studies as well as all synthetic procedures can be found in the Supporting Information.

ASSOCIATED CONTENT

Supporting Information

Details of the kinetic experiments, evaluation of the microscopic rate constants, synthetic procedures and product studies, as well as NBO calculation for cation **6**. This material is available free of charge via the Internet at http://pubs.acs.org.

AUTHOR INFORMATION

Corresponding Author

herbert.mayr@cup.uni-muenchen.de

Notes

The authors declare no competing financial interest.

ACKNOWLEDGMENTS

Dedicated to Professor Sema L. Ioffe on the occasion of his 75th birthday. We thank the Deutsche Forschungsgemeinschaft (Ma 673/22-1) for financial support. We are grateful to Anna Antipova, Ian Dunn, and Dr. Armin R. Ofial for their help during preparation of this manuscript as well as to Tobias A. Nigst for providing a sample of **12** and to Johannes Ammer for helpful discussions. We also thank Prof. Dr. Paul Knochel for his valuable suggestions concerning synthesis of optically active **3** and **4**.

REFERENCES

(1) Kotke, M.; Schreiner, P. R. (Thio)urea organocatalysts. In *Hydrogen Bonding in Organic Synthesis*; Pihko, P. M., Ed.; Wiley: Weinheim, 2009.

(2) Phipps, R. J.; Hamilton, G. L.; Toste, F. D. *Nat. Chem.* **2012**, *4*, 603−614.

(3) Dolling, U.-H.; Davis, P.; Grabowski, E. J. J. *J. Am. Chem. Soc.* **1984**, *106*, 446−447.

(4) (a) Ooi, T.; Maruoka, K. *Angew. Chem., Int. Ed.* **2007**, *46*, 4222−4266. (b) *Asymmetric Phase Transfer Catalysis*; Maruoka, K., Ed.; Wiley: Weinheim, 2008.

(5) For reviews on use of chiral Brønsted acids see, for instance: (a) Akiyama, T. *Chem. Rev.* **2007**, *107*, 5744−5758. (b) Rueping, M.; Nachtsheim, B. J.; Ieawsuwan, W.; Atodiresei, I. *Angew. Chem., Int. Ed.* **2011**, *50*, 6706−6720.

(6) (a) Nakashima, D.; Yamamoto, H. *J. Am. Chem. Soc.* **2006**, *128*, 9626−9627. (b) Jiao, P.; Nakashima, D.; Yamamoto, H. *Angew. Chem., Int. Ed.* **2008**, *47*, 2411−2413.

(7) (a) Rueping, M.; Ieawsuwan, W.; Antonchick, A. P.; Nachtsheim, B. J. *Angew. Chem., Int. Ed.* **2007**, *46*, 2097−2100. (b) Müller, S.; List, B. *Angew. Chem., Int. Ed.* **2009**, *48*, 9975−9978.

(8) Rueping, M.; Nachtsheim, B. J.; Moreth, S. A.; Bolte, M. *Angew. Chem., Int. Ed.* **2008**, *47*, 593−596.

(9) Rueping, M.; Uria, U.; Lin, M.-Y.; Atodiresei, I. *J. Am. Chem. Soc.* **2011**, *133*, 3732−3735.

(10) Hoffmann, S.; Seayad, A. M.; List, B. *Angew. Chem., Int. Ed.* **2005**, *44*, 7424−7427.

(11) Rueping, M.; Theissmann, T.; Kuenkel, A.; Koenigs, R. M. *Angew. Chem., Int. Ed.* **2008**, *47*, 6798−6801.

(12) Fleischmann, M.; Drettwan, D.; Sugiono, E.; Rueping, M.; Gschwind, R. M. *Angew. Chem., Int. Ed.* **2011**, *50*, 6364−6369.

(13) (a) Ratjen, L.; Müller, S.; List, B. *Nachr. Chem.* **2010**, *58*, 640−646. (b) Mahlau, M.; List, B. *Isr. J. Chem.* **2012**, *52*, 630−638.

(14) See, for instance: (a) Mayer, S.; List, B. *Angew. Chem., Int. Ed.* **2006**, *45*, 4193−4195. (b) Martin, N. J. A.; List, B. *J. Am. Chem. Soc.* **2006**, *128*, 13368−13369. (c) Wang, X.; List, B. *Angew. Chem., Int. Ed.* **2008**, *47*, 1119−1122.

(15) (a) Llewellyn, D. B.; Adamson, D.; Arndtsen, B. A. *Org. Lett.* **2000**, *2*, 4165−4168. (b) Hamilton, G. L.; Kang, E. J.; Mba, M.; Toste, F. D. *Science* **2007**, *317*, 496−499. (c) LaLonde, R. L.; Wang, Z. J.; Mba, M.; Lackner, A. D.; Toste, F. D. *Angew. Chem., Int. Ed.* **2010**, *49*, 598−601. (d) Rauniyar, V.; Wang, Z. J.; Burks, H. E.; Toste, F. D. *J. Am. Chem. Soc.* **2011**, *133*, 8486−8489. (e) Liao, S.; List, B. *Angew. Chem., Int. Ed.* **2010**, *49*, 628−631. It should be noted that in some cases the chiral phosphate may act as ligand and not as counterion for the cationic metal complex. Transformations where phosphate ions were shown to act as ligands are, for instance: (f) Mukherjee, S.; List, B. *J. Am. Chem. Soc.* **2007**, *129*, 11336−11337. (g) Jiang, G.; Halder, R.; Fang, Y.; List, B. *Angew. Chem., Int. Ed.* **2011**, *50*, 9752−9755.

(16) Ohmatsu, K.; Ito, M.; Kunieda, K.; Ooi, T. *Nat. Chem.* **2012**, *4*, 473−477.

(17) Macchioni, A. *Chem. Rev.* **2005**, *105*, 2039−2074 and references therein.

(18) (a) Raheem, I. T.; Thiara, P. S.; Peterson, E. A.; Jacobsen, E. N. *J. Am. Chem. Soc.* **2007**, *129*, 13404−13405. (b) Knowles, R. R.; Lin, S.; Jacobsen, E. N. *J. Am. Chem. Soc.* **2010**, *132*, 5030−5032. (c) Brown, A. R.; Kuo, W.-H.; Jacobsen, E. N. *J. Am. Chem. Soc.* **2010**, *132*, 9286−9288.

(19) (a) Xu, H.; Zuend, S. J.; Woll, M. G.; Tao, Y.; Jacobsen, E. N. *Science* **2010**, *327*, 986−990. (b) Uraguchi, D.; Ueki, Y.; Ooi, T. *Science* **2009**, *326*, 120−123.

(20) Bochmann, M. *Acc. Chem. Res.* **2010**, *43*, 1267−1278.

(21) (a) Young, W. G.; Winstein, S.; Goering, H. L. *J. Am. Chem. Soc.* **1951**, *73*, 1958−1963. (b) Winstein, S.; Schreiber, K. C. *J. Am. Chem. Soc.* **1952**, *74*, 2165−2170. (c) Winstein, S.; Schreiber, K. C. *J. Am. Chem. Soc.* **1952**, *74*, 2171−2178.

(22) Raber, D. J.; Harris, J. M.; Schleyer, P. v. R. In *Ions and Ion Pairs in Organic Reactions*, Vol. 2; Szwarc, M., Ed.; Wiley: New York, 1974.

(23) (a) De La Mare, P. B. D.; Vernon, C. A. *J. Chem. Soc.* **1954**, 2504−2510. (b) Sneen, R. A. *J. Am. Chem. Soc.* **1960**, *82*, 4261−4269. (c) Jia, Z. S.; Ottosson, H.; Zeng, X.; Thibblin, A. *J. Org. Chem.* **2002**, *67*, 182−187.

(24) Smith, M. B.; March, J. *March's Advanced Organic Chemistry*, 6th ed.; Wiley: Hoboken, NJ, 2007; p 470.

(25) Goering, H. L.; Blanchard, J. P.; Silversmith, E. F. *J. Am. Chem. Soc.* **1954**, *76*, 5409−5418.

(26) Goering, H. L.; Silversmith, E. F. *J. Am. Chem. Soc.* **1955**, *77*, 1129−1133.

(27) (a) Goering, H. L.; Silversmith, E. F. *J. Am. Chem. Soc.* **1955**, *77*, 6249−6253. (b) Goering, H. L.; Takahashi Doi, J. *J. Am. Chem. Soc.* **1960**, *82*, 5850−5854.

(28) Goering, H. L.; Nevitt, T. D.; Silversmith, E. F. *J. Am. Chem. Soc.* **1955**, *77*, 5026−5032.

(29) (a) Goering, H. L.; Koermer, G. S.; Linsay, E. C. *J. Am. Chem. Soc.* **1971**, *93*, 1230−1234. (b) The importance of conformational factors for 5-methylcyclohex-2-enyl system has been demonstrated: Goering, H. L.; Josephson, R. R. *J. Am. Chem. Soc.* **1962**, *84*, 2779−2785.
(30) Winstein, S.; Klinedinst, P. E., Jr.; Robinson, G. C. *J. Am. Chem. Soc.* **1961**, *83*, 885−895.
(31) Peters, K. S. *Chem. Rev.* **2007**, *107*, 859−873 and references therein.
(32) Yabe, T.; Kochi, J. K. *J. Am. Chem. Soc.* **1992**, *114*, 4491−4500.
(33) (a) Hammett, L. P. *Physical Organic Chemistry*, 2nd ed.; McGraw-Hill: New York, 1970. (b) Bentley, T. W; Schleyer, P. v. R. *Adv. Phys. Org. Chem.* **1977**, *14*, 1−67.
(34) Richard, J. P.; Jencks, W. P. *J. Am. Chem. Soc.* **1984**, *106*, 1383−1396.
(35) Richard, J. P.; Jencks, W. P. *J. Am. Chem. Soc.* **1984**, *106*, 1373−1383.
(36) (a) Tsuji, Y.; Mori, T.; Richard, J. P.; Amyes, T. L.; Fujio, M.; Tsuno, Y. *Org. Lett.* **2001**, *3*, 1237−1240. (b) Teshima, M.; Tsuji, Y.; Richard, J. P. *J. Phys. Org. Chem.* **2010**, *23*, 730−734.
(37) Schaller, H. F.; Tishkov, A. A.; Feng, X.; Mayr, H. *J. Am. Chem. Soc.* **2008**, *130*, 3012−3022.
(38) Minegishi, S.; Kobayashi, S.; Mayr, H. *J. Am. Chem. Soc.* **2004**, *126*, 5174−5181.
(39) For a review on carbocation−nucleophile combination reactions, see: Mayr, H.; Ofial, A. R. *J. Phys. Org. Chem.* **2008**, *21*, 584−595.
(40) For review on solvolysis reactions, see: Streidl, N.; Denegri, B.; Kronja, O.; Mayr, H. *Acc. Chem. Res.* **2010**, *43*, 1537−1549.
(41) (a) Mayr, H.; Ofial, A. R. *Pure Appl. Chem.* **2009**, *81*, 667−683. (b) Horn, M.; Mayr, H. *J. Phys. Org. Chem.* **2012**, *25*, 979−988.
(42) Ammer, J.; Sailer, C. F.; Riedle, E.; Mayr, H. *J. Am. Chem. Soc.* **2012**, *134*, 11481−11494.
(43) Ammer, J.; Nolte, C.; Mayr, H. *J. Am. Chem. Soc.* **2012**, *134*, 13902−13911.
(44) Troshin, K.; Schindele, C.; Mayr, H. *J. Org. Chem.* **2011**, *76*, 9391−9408.
(45) (a) Roos, G. H. P.; Donovan, R. A. *Synlett* **1996**, 1189−1190. (b) Johnson, R.; Sharpless, K. B. In *Catalytic Asymmetric Synthesis*, 2nd ed.; Ojima, I., Ed.; Wiley: New York, 2000; pp 231−280.
(46) Easton, A. M.; Habib, M. J. A.; Park, J.; Watts, W. E. *J. Chem. Soc., Perkin Trans. 2* **1972**, 2290−2297.
(47) (a) Grunwald, E.; Winstein, S. *J. Am. Chem. Soc.* **1948**, *70*, 846−854. (b) Bentley, T. W.; Carter, G. E. *J. Am. Chem. Soc.* **1982**, *104*, 5741−5747. (c) Kevill, D. N.; D'Souza, M. J. *J. Chem. Res.* **2008**, 61−66.
(48) Åkerlöf, G. *J. Am. Chem. Soc.* **1932**, *54*, 4125−4139.
(49) The half-reaction times were calculated as $t_{1/2} = (\ln 2)/k$, where k is the pseudo-first-order rate constant obtained by fitting $[(R)\text{-}\mathbf{1}]_t$ to the monoexponential function $\ln [(R)\text{-}\mathbf{1}]_t = -kt + \text{const}$. In the case of 90% aqueous acetone, only first 40 h of the reaction were evaluated, because re-isomerization of **2** which is formed during the reaction caused upward drifts in the $\ln [(R)\text{-}\mathbf{1}]_t$ vs t plot (see Supporting Information for details).
(50) As discussed in detail below, eq 11 predicts a second-order rate constant of 1.5×10^9 M^{-1} s^{-1} for the reaction of cation **6** with piperidine (N = 18.44, s_N = 0.44 for piperidine in water and E = 2.70 for **6**). An up-to-date database of reactivity parameters E, N, and s_N can be found at www.cup.lmu.de/oc/mayr/DBintro.html.
(51) Whereas 1,6-dibenzyl-1,2,3,4,5,6-hexahydro-1,3a,6,8-tetraazaphenalene was found to be the most universal photo-leaving group among a series of variously substituted aminopyridines (Nigst, T. A; Ammer, J.; Mayr, H. *J. Phys. Chem. A* **2012**, *116*, 8494−8499) its non-benzylated analogue can also be used as well in the present case, as the Lewis acidity of cation **6** is high enough to form stable pyridinium salts with both pyridines.
(52) Goering and Winstein differentiate between *external return*, i.e., the reaction between an added common anion and the free or paired carbocation, which results in the isotope exchange between the substrate and ^{14}C-labeled 4-nitrobenzoic acid, and *external ion pair return*, i.e., recombination of the SSIP, which can be suppressed by the addition of strong nucleophiles but does not result in the exchange with isotope-labeled 4-nitrobenzoic acid. As the participation of the SSIPs does not play a significant role in the present case, effects related to *external ion pair return* will be neglected.
(53) Dvorko, G. F.; Ponomareva, E. A. *Russ. J. Gen. Chem.* **2010**, *80*, 1615−1625 and references therein.
(54) Kantner, S. S.; Humski, K.; Goering, H. L. *J. Am. Chem. Soc.* **1982**, *104*, 1693−1697.
(55) Thibblin, A. *J. Chem. Soc., Perkin Trans. 2* **1987**, 1629−1632.
(56) Tsuji, Y.; Richard, J. P. *Chem. Rec.* **2005**, *5*, 94−106.
(57) The detailed description of the evaluation procedure can be found on pp S58−S95 of the Supporting Information.
(58) McClelland, R. A.; Kanagasabapathy, V. M.; Banait, N. S.; Steenken, S. *J. Am. Chem. Soc.* **1989**, *111*, 3966−3972.
(59) Denegri, B.; Minegishi, S.; Kronja, O.; Mayr, H. *Angew. Chem., Int. Ed.* **2004**, *43*, 2302−2305.
(60) Mayr, H.; Bug, T.; Gotta, M. F.; Hering, N.; Irrgang, B.; Janker, B.; Kempf, B.; Loos, R.; Ofial, A. R.; Remennikov, G.; Schimmel, H. *J. Am. Chem. Soc.* **2001**, *123*, 9500−9512.
(61) Atkins, P.; de Paula, J. *Atkins' Physical Chemistry*, 9th ed.; Oxford University Press: Oxford, 2010; p 840.
(62) More decimals of k_{-1}/k_2 and k'_{-1}/k_2 than given in Scheme 5 were used.
(63) While we do not have quantitative evidence for this assumption, picosecond dynamics of laser flash photolytically generated carbenium ions provide qualitative confirmation of it, as the ratio of rates of geminate recombination (corresponding to k_{-1}) and diffusional separation (corresponding to k_2) of photolytically generated ion pairs was reported to increase with increasing reactivity of the carbocation in the ion pair (see refs 32 and 42).
(64) Sailer, C.; Ammer, J.; Riedle, E.; Mayr, H., unpublished results.
(65) It should be noted that p_{ER} reflects the probability that a free carbenium ion **10** is captured by $^-$OPNB and not by the solvent. The probability that CIP generated by ionization of **10**-OPNB gives rise to a rearranged product via external return (e.g., (*S*)-**10**-OPNB from (*R*)-**10**-OPNB) is given by $0.5(1 - p_{IR}/100\%)p_{ER}$. This expression subtracts the fraction of CIPs consumed by internal return and multiplies with 0.5 to account for the fact that in the case of symmetrical allyl cations 50% of external return regenerates the starting material. As p_{IR} and p_{ER} do not correspond to competing processes, the sum of these terms can also be greater than 100%.
(66) Minegishi, S.; Loos, R.; Kobayashi, S.; Mayr, H. *J. Am. Chem. Soc.* **2005**, *127*, 2641−2649.
(67) Goering, H. L.; Pombo, M. M.; McMichael, K. D. *J. Am. Chem. Soc.* **1963**, *85*, 965−970.
(68) Troshin, K.; Mayr, H.; Mayer, P. *Acta Crystallogr., Sect. E: Struct. Rep. Online* **2012**, *68*, o2549.
(69) Hayashi, T.; Yamamoto, A.; Yoshihiko, I.; Nishioka, E.; Miura, H.; Yanagi, K. *J. Am. Chem. Soc.* **1989**, *111*, 6301−6311.
(70) De Rycke, N.; Berionni, G.; Couty, F.; Mayr, H.; Goumont, R.; David, O. R. P. *Org. Lett.* **2011**, *13*, 530−533.